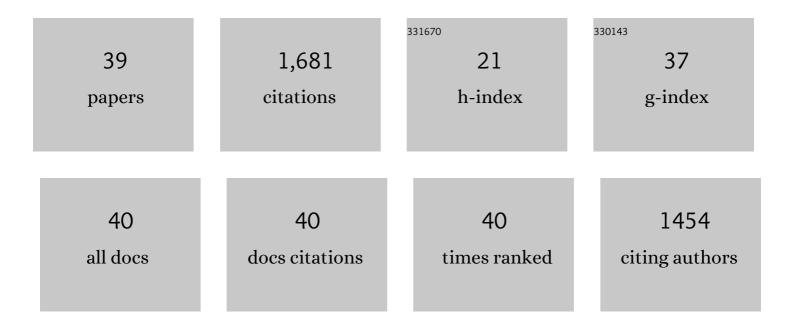
Song Gao

List of Publications by Year in descending order

Source: https://exaly.com/author-pdf/2112443/publications.pdf Version: 2024-02-01



SONC CAO

#	Article	IF	CITATIONS
1	Highly Morphologyâ€Controllable and Highly Sensitive Capacitive Tactile Sensor Based on Epidermisâ€Dermisâ€Inspired Interlocked Asymmetricâ€Nanocone Arrays for Detection of Tiny Pressure. Small, 2020, 16, e1904774.	10.0	166
2	Anodized Aluminum Oxide-Assisted Low-Cost Flexible Capacitive Pressure Sensors Based on Double-Sided Nanopillars by a Facile Fabrication Method. ACS Applied Materials & Interfaces, 2019, 11, 48594-48603.	8.0	130
3	Recent Advances in Carbon Materialâ€Based Multifunctional Sensors and Their Applications in Electronic Skin Systems. Advanced Functional Materials, 2021, 31, 2104288.	14.9	116
4	A high-accuracy, real-time, intelligent material perception system with a machine-learning-motivated pressure-sensitive electronic skin. Matter, 2022, 5, 1481-1501.	10.0	104
5	Structural Color Filters Enabled by a Dielectric Metasurface Incorporating Hydrogenated Amorphous Silicon Nanodisks. Scientific Reports, 2017, 7, 2556.	3.3	101
6	Artificial Optoelectronic Synapses Based on TiN <i>_x</i> O _{2–} <i>_x</i> MoS ₂ Heterojunction for Neuromorphic Computing and Visual System. Advanced Functional Materials, 2021, 31, 2101201.	14.9	92
7	Sn3O4/rCO heterostructure as a material for formaldehyde gas sensor with a wide detecting range and low operating temperature. Sensors and Actuators B: Chemical, 2020, 312, 127954.	7.8	85
8	Microâ€Nano Processing of Active Layers in Flexible Tactile Sensors via Template Methods: A Review. Small, 2021, 17, e2100804.	10.0	82
9	Highly reflective subtractive color filters capitalizing on a silicon metasurface integrated with nanostructured aluminum mirrors. Laser and Photonics Reviews, 2017, 11, 1600285.	8.7	74
10	Nanostructured perovskites for nonvolatile memory devices. Chemical Society Reviews, 2022, 51, 3341-3379.	38.1	71
11	Carbon-based nanomaterials for the detection of volatile organic compounds: A review. Carbon, 2021, 180, 274-297.	10.3	67
12	Ultrafast-response/recovery capacitive humidity sensor based on arc-shaped hollow structure with nanocone arrays for human physiological signals monitoring. Sensors and Actuators B: Chemical, 2021, 334, 129637.	7.8	58
13	Twofold Polarizationâ€Selective Allâ€Dielectric Trifoci Metalens for Linearly Polarized Visible Light. Advanced Optical Materials, 2019, 7, 1900883.	7.3	55
14	Subtractive Color Filters Based on a Silicon-Aluminum Hybrid-Nanodisk Metasurface Enabling Enhanced Color Purity. Scientific Reports, 2016, 6, 29756.	3.3	53
15	Structural color filters based on an all-dielectric metasurface exploiting silicon-rich silicon nitride nanodisks. Optics Express, 2019, 27, 667.	3.4	49
16	All-dielectric metasurfaces for simultaneously realizing polarization rotation and wavefront shaping of visible light. Nanoscale, 2019, 11, 4083-4090.	5.6	40
17	High-Performance Formaldehyde Gas Sensor Based on Cu-Doped Sn ₃ O ₄ Hierarchical Nanoflowers. IEEE Sensors Journal, 2020, 20, 6945-6953.	4.7	31
18	Aluminum Plasmonic Metasurface Enabling a Wavelength-Insensitive Phase Gradient for Linearly Polarized Visible Light. ACS Photonics, 2017, 4, 322-328.	6.6	29

Song Gao

#	Article	IF	CITATIONS
19	A Highly Efficient Bifunctional Dielectric Metasurface Enabling Polarizationâ€Tuned Focusing and Deflection for Visible Light. Advanced Optical Materials, 2019, 7, 1801337.	7.3	29
20	A waterproof and breathable Cotton/rGO/CNT composite for constructing a layer-by-layer structured multifunctional flexible sensor. Nano Research, 2022, 15, 9341-9351.	10.4	26
21	Study on Multilevel Resistive Switching Behavior With Tunable ON/OFF Ratio Capability in Forming-Free ZnO QDs-Based RRAM. IEEE Transactions on Electron Devices, 2020, 67, 4884-4890.	3.0	24
22	Allâ€Dielectric Fiber Metaâ€Tip Enabling Vortex Generation and Beam Collimation for Optical Interconnect. Laser and Photonics Reviews, 2021, 15, 2000581.	8.7	21
23	Efficient All-Dielectric Diatomic Metasurface for Linear Polarization Generation and 1-Bit Phase Control. ACS Applied Materials & Interfaces, 2021, 13, 14497-14506.	8.0	20
24	A Digital–Analog Integrated Memristor Based on a ZnO NPs/CuO NWs Heterostructure for Neuromorphic Computing. ACS Applied Electronic Materials, 2022, 4, 3525-3534.	4.3	18
25	Angle-tolerant linear variable color filter based on a tapered etalon. Optics Express, 2017, 25, 2153.	3.4	17
26	Polarization-encrypted high-resolution full-color images exploiting hydrogenated amorphous silicon nanogratings. Nanophotonics, 2020, 9, 875-884.	6.0	15
27	Multifunctional Optoelectronic Random Access Memory Device Based on Surfaceâ€Plasmaâ€Treated Inorganic Halide Perovskite. Advanced Electronic Materials, 2021, 7, 2100366.	5.1	15
28	Vertically integrated visible and near-infrared metasurfaces enabling an ultra-broadband and highly angle-resolved anomalous reflection. Nanoscale, 2018, 10, 12453-12460.	5.6	14
29	Reusable, Non-Invasive, and Ultrafast Radio Frequency Biosensor Based on Optimized Integrated Passive Device Fabrication Process for Quantitative Detection of Glucose Levels. Sensors, 2020, 20, 1565.	3.8	13
30	Dielectric metasurfaces based on a rectangular lattice of a-Si:H nanodisks for color pixels with high saturation and stability. Optics Express, 2019, 27, 35027.	3.4	13
31	All Dielectric Transmissive Structural Multicolor Pixel Incorporating a Resonant Grating in Hydrogenated Amorphous Silicon. Scientific Reports, 2017, 7, 13574.	3.3	12
32	Dielectric Polarizationâ€Filtering Metasurface Doublet for Trifunctional Control of Full‧pace Visible Light. Laser and Photonics Reviews, 2022, 16, .	8.7	11
33	Multifunctional Beam Manipulation at Telecommunication Wavelengths Enabled by an Allâ€Dielectric Metasurface Doublet. Advanced Optical Materials, 2020, 8, 2000645.	7.3	10
34	High-performance and self-rectifying resistive random access memory based on SnO ₂ nanorod array: ZnO nanoparticle structure. Applied Physics Express, 2019, 12, 121002.	2.4	6
35	Linear variable filter enabling an enhanced wavelength gradient based on shadowâ€mask sputtering. Microwave and Optical Technology Letters, 2017, 59, 3142-3146.	1.4	4
36	Prediction of Glucose Concentration in a Glucose-Lactose Mixture Based on the Reflective Optical Power at Dual Probe Wavelengths. Journal of the Optical Society of Korea, 2016, 20, 199-203.	0.6	2

#	Article	IF	CITATIONS
37	Design of Broadband LNA and RFVGA for DVB Receiver Tuner using CMOS \$0.18-mumathrm{m}\$ Process. , 2019, , .		1
38	Multifunctional Metasurfaces: Twofold Polarizationâ€Selective Allâ€Dielectric Trifoci Metalens for Linearly Polarized Visible Light (Advanced Optical Materials 21/2019). Advanced Optical Materials, 2019, 7, 1970082.	7.3	0
39	Metasurface Doublet: Multifunctional Beam Manipulation at Telecommunication Wavelengths Enabled by an Allâ€Dielectric Metasurface Doublet (Advanced Optical Materials 15/2020). Advanced Optical Materials, 2020, 8, 2070062.	7.3	0